ORIGINAL ARTICLE

Gene expression profiles of giant hairy naevi

M R K Dasu, R E Barrow, H K Hawkins, R L McCauley

J Clin Pathol 2004;**57**:849–855. doi: 10.1136/jcp.2003.014274

See end of article for authors' affiliations

Correspondence to: Dr M R K Dasu, Shriners Hospitals for Children, 815 Market Street, Galveston, TX 77550, USA; drmohan@utmb.edu

Accepted for publication 8 March 2004

Background: Congenital neomelanocytic naevi appear in nearly 1% of newborns. Giant hairy naevi (GHN) are uncommon lesions covering large areas of the body. They are of concern because they have the potential to transform into malignant melanomas.
Aims: To describe gene expression profiles of GHN and nearby normal skin from patients with GHN and normal control skin (from patients with cleft lip/palate).
Methods: Tissues from three patients with GHN and two normal controls were studied for differences in gene expression profiles. Total RNA was isolated from normal skin near the hairy naevus, GHN, and skin from normal controls. The RNA samples were subjected to probe labelling, hybridisation to chips, and image acquisition according to the standard Affymetrix protocol.
Results: There were 227 genes affected across all samples, as determined by DNA microarray analysis. There was increased expression of 22 genes in GHN compared with nearby normal skin. Decreased expression was noted in 73 genes. In addition, there was increased expression of 36 genes in normal skin near GHN compared with normal control skin, and decreased expression of five genes. Categories of genes affected were those encoding structural proteins, proteins related to developmental processes, cell death associated proteins, transcription factors, growth factors, stress response modulators, and collagen associated proteins. Changes in mRNA expression were checked by reverse transcription polymerase chain reaction.
Conclusions: Genetic profiles of GHN may provide insight into their pathogenesis, including their potential for malignant transformation. Such information may be useful in improving the understanding and management of these lesions.

Congenital neomelanocytic naevi appear in nearly 1% of all newborn infants. Most of these naevi are small; however, a special group of melanocytic lesions cover large areas of the body. These large lesions, termed giant hairy naevi (GHN), are of concern because they have the potential to transform into malignant melanomas, with an incidence of 1% to 25%.[1–8] The malignant melanoma that develops within other naevi typically begins at the epidermal–dermal junction, whereas in a GHN, malignant melanoma originates deep in the dermis.[1 7] Giant hairy naevi are relatively uncommon congenital malformations that are usually deeply pigmented, covered with a moderate growth of hair, and occur over large areas of the body. They represent developmental lesions arising from migratory arrest and proliferation of primitive neuroectodermal cells.[9] The available evidence suggests that neoplasms arising in this setting are diverse in their morphological expression and variable in their clinical behaviour.[10] Because most of these lesions are treated early, for cosmetic reasons and because of their malignant potential, the true incidence of malignant degeneration is unknown.

> ''Gene expression profiling by microarrays represents a valuable tool to identify new players in complex pathophysiological processes, such as melanoma''

Oligonucleotide or cDNA arrays have dramatically changed the study of the pattern of gene expression by enabling the simultaneous analysis of thousands of genes in a single experiment. For this reason, gene expression profiling by microarrays represents a valuable tool to identify new players in complex pathophysiological processes, such as melanoma.[11–13]

In our study, gene expression profiles are described in GHN and the nearby normal skin of patients with GHN, in comparison with the normal skin of unaffected patients. Gene expression profiling in these lesions may provide insight into the pathogenesis of GHN, and perhaps into the biological potential of individual lesions.

METHODS

Patients and study design

Tissues from three patients with GHN and two patients with cleft lip and cleft palate (normal controls) were studied. The patients ranged in age from 2 to 22 years, and were admitted to our hospital for the removal of giant hairy naevi or for reconstructive surgery. Samples of tissue were taken during planned surgical procedures from GHN, from apparently normal skin near to the hairy naevus, and from the normal skin of patients admitted for the reconstruction of a cleft lip or cleft palate, in accordance with an IRB approved protocol. The samples were taken from the elbow, face, and back of the trunk. Samples were snap frozen and stored at −70℃ for DNA microarray analysis and reverse transcription polymerase chain reaction (RT-PCR) analysis. Patterns of mRNA expression were compared between GHN and nearby normal skin, and between the normal skin near the GHN and the normal skin of control patients without such naevi. Figure 1 depicts an example of a GHN involving large areas of the trunk and legs.

Total RNA extraction

Total RNA was isolated from the frozen tissue samples by acid guanidinium thiocyanate/phenol/chloroform extraction using TRI® reagent (Molecular Research Center Inc, Cincinnati, Ohio, USA). This method was based on the single

Abbreviations: GHN, giant hairy naevi; HIF, hypoxia inducible factor; RT-PCR, reverse transcriptase polymerase chain reaction; TRP-1, tyrosinase related protein 1; TRP-2, tyrosinase related protein or dopachrome tautomerase; VEGF, vascular endothelial growth factor

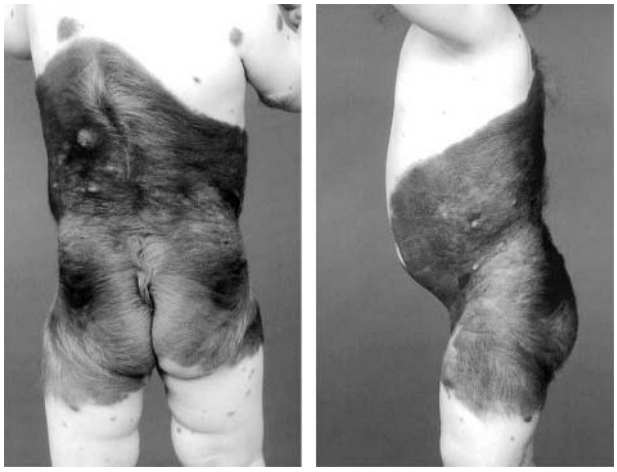

Figure 1 Child (2 years old) with a giant hairy naevus covering the back, legs, and abdomen.

step method of RNA isolation described by Chomczynski and Sacchi.[14] Samples were homogenised in TRI® reagent on ice and total RNA was extracted according to the manufacturer's instructions. Purified RNA was measured by ultraviolet absorbance at 260 and 280 nm and stored in 25 μg aliquots at −70℃ for DNA microarray hybridisation and analyses. The adequacy and integrity of the extracted RNA were determined by gel electrophoresis.

High density oligonucleotide array analysis

Probe labelling, hybridisation, and image acquisition were done according to the standard Affymetrix protocol. Briefly, 25 μg samples of purified total RNA were transcribed into cRNA, purified, and used as templates for the in vitro transcription of biotin labelled antisense RNA. The biotinylated antisense RNA preparation was fragmented, and placed in a hybridisation mixture containing four biotinylated hybridisation controls (BioB, BioC, BioD, and Cre). Eight samples (three GHN, three nearby normal skin of patients with GHN, and two normal controls) were then hybridised to eight Affymetrix gene chip arrays (HG-U95 Av2, from identical lots) for 16 hours. The arrays were washed and stained using the instrument's standard eukaryotic GE wash 2′ protocol and antibody mediated signal amplification. The images were scanned and analysed with Afffymetrix GeneChip analysis suite 5.0. Images from each gene chip were scaled and adjusted to an average intensity value for all arrays of 1500. Scaled average difference values and absolute call data from each gene chip were exported to data files and used for statistical analysis.[15 16] A probe is ''present'' if its absolute call was ''P'' for at least two members of the group containing all samples. Otherwise, the gene was considered not expressed in the group using the Affymetrix algorithm. In vitro transcription and chip hybridisation were performed in collaboration with the UTMB Genomic Core Facility.

Data analysis

Data analysis was carried out as described previously, including: chip validation, normalisation, filtering of data, and generation of gene lists by comparing (1) GHN and nearby normal skin, and (2) the normal skin near the GHN and normal skin of control patients without such naevi.[15] The first step was to determine the degree of similarity or dissimilarity among sample transcription profiles by using model based expression analysis of oligonucleotide arrays.[16] The next step was the elimination of genes that showed little variation across the samples, or that were absent in most of the samples. The first criterion was that the ratio of the SD and the mean of a gene's expression across all samples was less than the threshold (of 0.85 and the upper limit of 8). Data were discarded if there was a large deviation in the number of present calls or if the correlation coefficient among the three chips within the group was less than 0.85. The second criterion required a gene to be called present in more than 80% of the arrays. We determined the presence (P) or absence (A) of each probe within the group according to the Affymetrix algorithm. A probe is ''present'' if its absolute call was ''P'' for at least two members of the group containing all samples. Otherwise, the gene was considered not expressed in the group. The primary goal was to identify genes with significant differences in expression between the test and control groups. The within group average of expression was calculated and comparisons were made between groups. Initially, comparisons were done by computing the expression fold difference for each gene and listing those that showed more than 1.5 fold increases or decreases in activity. Three groups were used for comparison: one group consisted of tissue from GHN ($n = 3$), one consisted of nearby normal skin from patients with GHN ($n = 3$), and one was normal control skin from patients with cleft palate ($n = 2$). Paired comparisons were made between GHN and nearby normal skin, whereas unpaired comparisons were made between the uninvolved skin near to GHN and normal control skin. An entry was discarded as an outlier when its value was greater than 3 SD from the mean. Only significant differences at $p < 0.05$ were retained.[17] Considering the number of samples in each group and its influence on the validity of the analysis, the power of the *t* test was computed. If less than 0.8, results were discarded even when $p < 0.05$. By using HG-U95Av2 Affymetrix arrays, about 6000 of the 12 625 genes present in the array were expressed in all the chips.

RT-PCR

The amount of total RNA extracted from GHN and nearby normal skin was measured by ultraviolet spectrophotometry and the RNA was stored at −70℃ for RT-PCR analysis. The cDNA reaction and the PCR were performed with an optimised buffer and enzyme system (Titan™ One Tube RT-PCR system; Roche, Indianapolis, Indiana, USA). This system is designed to use avian myeloblastosis virus (AMV) reverse transcriptase for first strand synthesis and the Expand™ high fidelity blend of thermostable DNA polymerases, which consists of Taq DNA polymerase and a proof reading polymerase, for the PCR part. The reaction was carried out in a 50 μl volume containing 50–100 ng of total RNA, 1 μM of forward and reverse primers specific for hypoxia inducible factor 1 (HIF-1; GenBank Accession Number, U22431; forward: 5′-ACC CCA TTC CTC ACC CAT CA-3′ and reverse: 5′-TCC ACC TCT TTT GGC AAG C-3′), dopachrome tautomerase (TRP-2; GenBank Accession Number, AJ000503; forward: 5′-GGA GAA AAG TAC GAC AGA GAC AAG G-3′ and reverse: 5′-AGA AAA GCC AAC AGC ACA AAA AGA C-3′), and vascular endothelial growth factor (VEGF; primer pairs from R&D Systems, Minnesota, Minneapolis, USA); 1× PCR buffer with 4mM Mg^{2+}, 0.2mM dNTPs, 5mM dithiothreitol solution, 5–10 units of RNAse inhibitor, and 0.05 U/μl of the enzyme mix (High Fidelity enzyme mix, reverse transcriptase, AMV in storage buffer). An initial RT step was performed at 50℃ for 30 minutes and 94℃ for two minutes for one cycle, followed by 35 cycles of denaturation at 94℃ for 15 seconds, annealing at 55℃ for 30 seconds, and extension at 72℃ for 1.5 minutes, with a final extension step of 72℃ for five minutes. In addition, primers for human β actin were used (R&D systems) as a ''house

keeping gene'' to provide an internal marker for mRNA integrity within the experiment. PCR products were separated on (1.5% wt/vol) agarose gels, and visualised by means of ethidium bromide staining under ultraviolet light. Image capture and density analysis of bands were done with the SynGene™ gel documentation system (SynGene-Synoptics, Cambridge, UK) and the band intensity was expressed as the ratio of HIF-1 to β actin.[18]

Our study was conducted in compliance with the requirements for institutional review and informed consent at the University of Texas Medical Branch, Galveston, Texas, USA.

RESULTS

Histopathology

The diagnosis of GHN was confirmed histologically in each case. The dermal portions of the biopsies of the GHN were almost filled with moderate sized to small ''naevus cells'' with uniform ovoid nuclei, which are thought to represent immature melanocytic cells derived from the neural crest (fig 2A, B). Similar cells, which often were smaller and more elongated, extended to the deepest portion of the dermis. In the upper dermis, the cells had more cytoplasm, often forming rounded nests, and often contained finely granular brown cytoplasmic pigment. In some cases, nests of naevus cells were in contact with the dermal–epidermal junction. Multiple long hair follicles were present. The naevus cells made up just over 50% of the total number of cells. The other cells did not differ dramatically in their populations between GHN and normal skin, except for the macrophages, which were approximately two to fivefold more numerous in the naevi, and presumably more activated, by virtue of phagocytosis of melanin pigment. In general, the normal skin taken from patients with GHN was histologically identical to that from patients without GHN. There was the expected random variability in epidermal thickness and degree of pigmentation.

Gene expression patterns

After survey and statistical analysis of the 12 625 genes on each array, there was increased expression of 22 genes in the GHN tissue compared with the nearby normal skin, and a decrease in 73 genes (table 1). Thus, 0.75% of the genes were altered in GHN when compared with nearby normal skin. There were 227 genes that changed across all samples, as determined by microarray analysis, satisfying the filtering criteria as mentioned above. Categories of genes affected were those encoding structural proteins, proteins related to developmental processes, cell death associated proteins, transcription factors, growth factors, stress response modulators, and collagen associated proteins. A comparison between the unaffected nearby normal skin of patients with GHN and normal control skin generated a list of genes, 36 of which had increased expression and five of which had decreased expression (table 2).

Confirmation by RT-PCR

To confirm the findings using a different methodology, the degree of expression of three genes (HIF-1, TRP-2, and VEGF) found to be significantly altered in GHN compared with nearby normal skin was analysed by RT-PCR. The ratio of TRP-2 mRNA to β actin in GHN was 4.32 (SD, 0.06), compared with 0.94 (SD, 0.11) in normal skin ($p < 0.05$). The ratio of HIF-1 mRNA to β actin in normal skin was 2.32 (SD, 0.06), compared with 0.74 (SD, 0.01) in GHN tissue, and the ratio of VEGF to β actin in normal skin was 3.64 (SD, 0.15), compared with 0.82 (SD, 0.2) in GHN ($p<0.05$), which corroborate the microarray data.

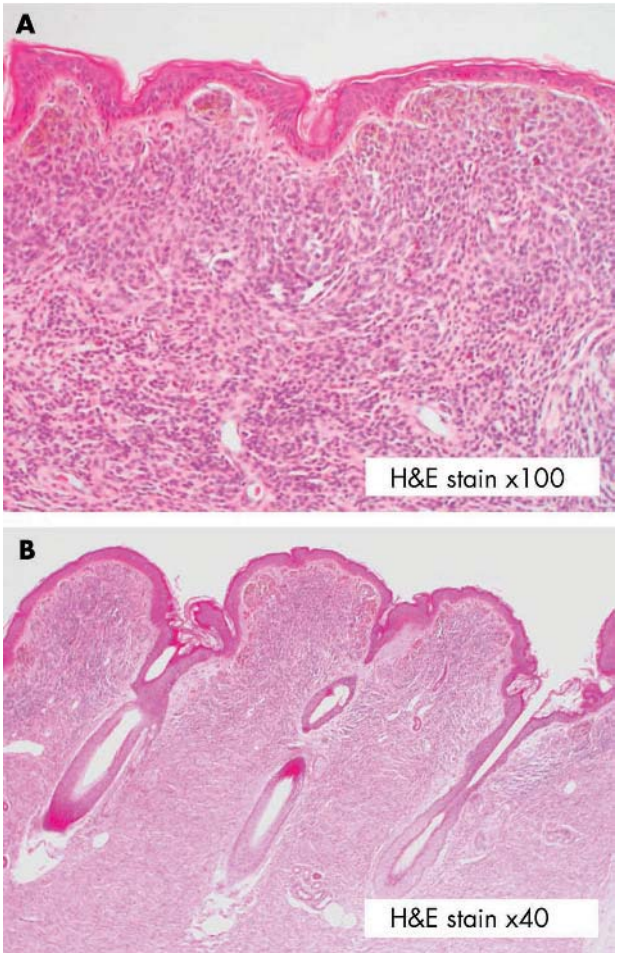

Figure 2 Light micrographs of giant hairy naevus. (A) Cells with orderly nuclei and scant cytoplasm occupy the entire dermis. Melanophages can be seen beneath the epidermis. Haematoxylin and eosin stain (H&E); original magnification, ×100. (B) At low magnification, large regularly spaced hair follicles are apparent. The dermis appears to be cellular and there are foci of pigmentation in the papillary dermis. H&E stain; original magnification, ×40.

DISCUSSION

Little information is currently available as to how changes in gene expression in the skin affect the development of GHN. New technology now allows us to investigate changes in gene expression using high density oligonucleotide microarrays in abnormal tissue such as GHN, in comparison with normal skin. Gene profiling may provide information on how these lesions develop and progress.

Comparison of the gene expression profile in GHN with the patient's own nearby normal skin showed that there was a significant increase in the expression of 22 genes and a decrease in the expression of 73 genes. These genes can be categorised into functional groups. As examples, TRP-2 (GenBank accession number, AJ000503) and tyrosinase related protein 1 (TRP-1; GenBank accession number, X51420) were significantly raised. Both of these are recognised as useful markers of melanoma, because expression of these genes is restricted to cells of melanocytic origin. Tyrosinase protein or its mRNA can be detected even in poorly differentiated amelanotic melanomas,[19–21] as documented at the ultrastructural level.[22] The relative abundance of tyrosinase mRNA in some undifferentiated amelanotic melanomas[19] allows its use in PCR techniques as a valuable diagnostic option.[20] The same can be said for the

Table 1 List of genes altered in giant hairy naevus (GHN) compared with normal skin from patients with GHN

Accession number	Gene	Significant fold change*	Function
AJ000503	Dopachrome tautomerase (Δ isomerase, TRP-2)	8.86	Melanoma marker
D00632	Glutathione peroxidase 3 (plasma)	6.76	Enzyme
X00734	Tubulin, β5	4.74	Structural protein
D50840	UDP-glucose ceramide glucosyltransferase	3.93	Enzyme
U87947	Epithelial membrane protein 3	3.63	Membrane protein
L26232	Phospholipid transfer protein	3.59	Transport protein
L05424	Cell surface glycoprotein CD44 gene	3.29	Immune response
X82153	Cathepsin K (pycnodysostosis)	3.23	Lysosomal enzyme
AF098641	CD44 isoform RC (CD44) mRNA	3.23	Immune response
AJ001183	SRY (sex determining region Y), box 10	3.15	Differentiation
AL021396	Hypothetical protein	3.01	Pathophysiology
J04430	Acid phosphatase 5, tartrate resistant (TRAP)	2.88	Metabolism and transport
M77348	Silver (Pmel 17, melanocyte specific gene)	2.88	Pigmentation gene
M59040	CD44 antigen	2.72	Immune response
U60060	Fasciculation and elongation protein, ζ1 (zygin I)	2.61	Cell signalling
AB011088	Sperm associated antigen 9	2.57	Development
D17547	Dopachrome tautomerase (Δ isomerase, TRP-2)	2.56	Melanoma marker
J03553	Human pulmonary surfactant protein (SP5) mRNA	2.40	Surfactant protein
AF035119	Deleted in liver cancer 1 (DLC1)	2.32	Tumour suppressor gene
AF072468	Jerky (mouse) homologue (JH8)	2.08	Epilepsy gene
AF044253	K^+ voltage gated channel, β member 2 (HKvβ2.2)	2.08	Signal transduction
X51420	Tyrosinase related protein 1 (TRP-1)	2.07	Melanoma marker
D45288	Expressed sequence tag	1.97	Unknown
X05276	Tropomyosin 4	−1.66	Structural protein
D31716	Basic transcription element binding protein 1	−1.75	Transcription
AW007731	Purine rich element binding protein B	−1.78	DNA binding
U22431	Hypoxia inducible factor 1, α subunit	−1.84	Stress response
X15804	Actinin, α1	−1.88	Structural protein
D87434	KIAA0247 gene product	−1.89	Unknown
S81439	Early growth response α	−1.90	Cell cycle regulation
AB023209	Palladin	−1.90	Protein folding
AL049288	Bladder cancer associated protein	−1.90	Protein marker
M28170	CD19 antigen	−1.92	B cell signalling
AJ224901	Zinc finger protein 198	−1.98	Cell signalling
U84011	Amylo-1,6-glucosidase, 4-α-glucanotransferase enzyme	−1.98	Glycogen debranching
U84487	SOCS-1 (fractalkine, neurotactin)	−1.99	Cell signalling
U94905	Diacylglycerol kinase, ζ (104 kDa) (DAG)	−2.01	Cell signalling
AB014511	ATPase, class II, type 9A	−2.04	Metabolism
AF041080	Hect domain and RLD 2	−2.11	Unknown
AI222594	Expressed sequence tag	−2.11	Unknown
X16663	Haemopoietic cell specific Lyn substrate 1	−2.12	B cell signalling
D13629	Kinectin 1 (kinesin receptor)	−2.12	Motor cargo proteins
AB005754	Lymphokine activated killer (LAK-1)	−2.12	Immune response
U85193	Nuclear factor I/B	−2.16	Stress response
L77886	Protein tyrosine phosphatase, receptor type, K	−2.18	Signal transduction
AL096780	Choline kinase like	−2.19	Metabolism
U82328	Pyruvate dehydrogenase complex	−2.20	Metabolism
D13639	Cyclin D2	−2.23	Cell cycle
M63193	Platelet derived endothelial cell growth factor 1(PD-EGF)	−2.23	Angiogenesis
AL021154	E2F transcription factor 2	−2.27	Cell cycle
AL050378	Expressed sequence tag	−2.28	Unknown
J00153	α Globin gene cluster on chromosome 16	−2.29	Metabolism
D29805	UDP-β-1,4-galactosyltransferase, polypeptide 1	−2.30	Growth and development
X77777	Vasoactive intestinal peptide receptor 1	−2.30	Growth and differentiation
AL049946	DKFZP564I1922 protein	−2.31	Unknown
AB022660	KIAA0437 protein	−2.32	Unknown
X02160	Insulin receptor	−2.32	Cell signalling
D61391	Phosphoribosyl pyrophosphate synthetase protein 1	−2.33	Metabolism
AB002298	KIAA0300 protein	−2.37	Unknown
AB029018	KIAA1095 protein	−2.39	Unknown
AI651806	Cysteine rich motor neurone 1	−2.43	Cell signalling
M64572	Protein tyrosine phosphatase, non-receptor type 3	−2.45	Signal transduction
AF052142	Expressed sequence tag	−2.50	Unknown
D64110	BTG family, member 3	−2.50	Cell growth and regulation
X05409	Aldehyde dehydrogenase 2, mitochondrial	−2.50	Metabolism
X62534	HMG protein 2 (HMGB2)	−2.52	DNA integration
AF056087	Secreted frizzled related protein 1 (hsFRP)	−2.67	Tumour suppressor
AF063002	Four and a half LIM domains 1 (FHL-1)	−2.72	Myogenesis
AF099989	Ste-20 related kinase	−2.75	Growth and differentiation
U90907	Expressed sequence tag	−2.76	Unknown
M25079	Haemoglobin β	−2.76	Metabolism
X99268	Twist (drosophila) homologue	−2.81	Transcription factor
M27492	Interleukin 1 receptor, type I	−2.85	Inflammatory response
U13616	Ankyrin 3, node of Ranvier (ankyrin G)	−2.87	Cell signalling
L13463	Regulator of G protein signalling 2, 24 kDa	−2.95	Signal transduction
AI687419	Expressed sequence tag	−2.96	Unknown
X59766	α-2 Glycoprotein 1, zinc	−3.01	Acute phase response
AF099935	Tumour necrosis factor induced protein	−3.18	Immune response
M26326	Keratin 18	−3.20	Structural protein
M31682	Inhibin, β-B (activin AB β polypeptide)	−3.26	Cell signalling

Table 1 Continued

Accession number	Gene	Significant fold change*	Function
U10550	GTP binding protein	−3.26	Cell signalling
U97519	Podocalyxin like	−3.78	Cell surface marker
U67156	Mitogen activated protein kinase kinase kinase 5	−3.78	Signal transduction
L06797	Chemokine (C-X-C motif), receptor 4 (fusin)	−3.84	Inflammatory response
AI445461	Transmembrane 4 superfamily member 1	−3.97	Membrane transport
U43626	γ-Aminobutyric acid (GABA) A receptor, ε	−4.90	Neurotransmitter
AJ238246	Keratin 7	−4.91	Structural protein
L11706	Lipase, hormone sensitive	−5.20	Metabolism
D78611	Mesoderm specific transcript (mouse) homologue	−5.22	Growth and differentiation
AF022375	Vascular endothelial growth factor (VEGF)	−5.70	Angiogenesis
D45371	Adipose most abundant gene transcript 1	−7.58	Metabolism
U76456	Tissue inhibitor of metalloproteinase 4	−8.60	Extracellular matrix
AA128249	Fatty acid binding protein 4, adipocyte	−8.75	Metabolism
X03350	Alcohol dehydrogenase 2 (class I), β polypeptide	−9.55	Metabolism
M12963	Alcohol dehydrogenase 1 (class I), α polypeptide	−12.05	Metabolism

*p<0.05 for GHN versus normal skin from a patient with GHN.

determination of TRP-1, recognised by the commercially available antibody MEL-5, and TRP-2, which acts as dopachrome tautomerase. Expression of these genes and proteins is found predominantly in cells of melanocytic lineage. Thus, identification of the protein tyrosinases, TRP-1 and TRP-2, and structural melanosomal proteins, collectively called melanogenesis related proteins, provides a highly specific and sensitive tool for the positive identification of melanocytes. Pocket proteins are thought to govern the G1 to S phase transition mainly through their interaction with E2F transcription factors. E2F transcription factor (GenBank accession number, AL021154) expression was significantly decreased in GHN. E2F regulates the transcription of a large set of genes involved in all aspects of S phase initiation and progression, such as the mcm genes, cyclin E, proliferating cell nuclear antigen, and DNA polymerase α. Alterations in

Table 2 List of genes altered in normal skin of individuals with giant hairy naevus (GHN) versus skin from normal controls

Accession number	Gene	Significant fold change*	Function
M84526	D component of complement (adipsin)	21.8	Immune response
X52022	Collagen, type VI, α3	14.2	Structural protein
M15856	Lipoprotein lipase	13.9	Metabolism
X07979	Integrin β1 subunit	10.1	Extracellular matrix
J03040	Osteonectin	9.3	Cell adhesion
L25286	Collagen, type XV, α1	8.7	Structural protein
XM_056455	Melanoma associated gene	8.5	Melanoma marker
X05610	Collagen, type IV, α2	8.5	Structural protein
U20982	Insulin-like growth factor binding protein 4 (IGFBP4)	8.4	Growth and differentiation
D10040	Fatty acid coenzyme A ligase, long chain 2	8.0	Metabolism
L19182	Insulin-like growth factor binding protein 7 (IGFBP7)	8.0	Growth and differentiation
M62403	Insulin-like growth factor binding protein 4 (IGFBP4)	7.9	Growth and differentiation
X05409	Aldehyde dehydrogenase 2 family (mitochondrial)	7.8	Metabolism
M33210	Human colony stimulating factor 1 receptor (CSF1R)	7.8	Immune response
X86693	SPARC-like 1 (mast 9, hevin)	7.7	Tissue remodelling
AL039458	Orthologue of mouse integral membrane glycoprotein LIG-1	6.9	Membrane glycoprotein
L11706	Lipase, hormone sensitive	6.8	Metabolism
M81945	Human CD34 gene, promoter and coding sequence	6.6	Immune response
L42373	Protein phosphatase 2, α isoform	6.5	Signal transduction
AL050159	DKFZP586A0522 protein	6.4	Unknown
AL049798	Dermatopontin	6.3	Extracellular matrix
X13839	Actin, α2, smooth muscle, aorta	6.0	Structural protein
J03278	Platelet derived growth factor receptor, β polypeptide	5.7	Cell growth
AI813532	Tumour necrosis factor receptor superfamily, member 1B	5.4	Immune response
U65093	Cbp/p300 interacting transactivator, 2	4.6	Proliferation and cell cycle
M95787	Transgelin	4.6	Gap junction protein
W27949	Chromosome 6 open reading frame 34 (BACH1)	4.2	Tumour suppressor gene
AF007150	Angiopoietin-like 2	4.1	Lipid metabolism
U67963	Lysophospholipase like	3.2	Lipid metabolism
U05861	Hepatic dihydrodiol dehydrogenase gene	3.1	Metabolism
D16294	Acetyl coenzyme A acyltransferase 2 (mitochondrial)	3.0	Metabolism
X02160	Insulin receptor	2.9	Cell signalling
X96752	L-3-hydroxyacyl coenzyme A dehydrogenase, short chain	2.6	Metabolism
U29091	Selenium binding protein 1	2.6	Peroxisome proliferation
L27560	Insulin-like growth factor binding protein 5 (IGFBP5)	2.6	Growth and differentiation
U72649	BTG family, member 2	2.4	Cell growth and regulation
AA181053	Parvin, β	−3.9	Cell matrix and adhesion
U72511	B cell associated protein	−4.3	Immune response
AA524547	FXYD domain containing ion transport regulator 1	−6.1	Membrane transport
N36638	Protein phosphatase 1, regulatory (inhibitor) subunit 3C	−7.0	Signal transduction
X00351	Actin, β	−23.7	Structural protein

*p<0.05 for normal skin with hairy naevus versus normal control skin

the cell cycle, DNA damage and repair, and tumour suppressor genes have been linked to the development of cancer. In GHN, two tumour suppressor genes were found to be altered. Deleted in liver cancer 1 (DLC1; GenBank accession number, AF035119) gene expression is increased, whereas secreted frizzled related protein 1 (hsFRP; GenBank accession number, AF056087) is decreased. HIF-1α (GenBank accession number, U22431) gene expression was decreased in GHN. HIF-1 is a transcription factor that functions as a master regulator of oxygen homeostasis. Over 40 HIF-1 target genes have been identified, which encode proteins that play key roles in crucial developmental and physiological processes, including angiogenesis/vascular remodelling, erythropoiesis, glucose transport, glycolysis, iron transport, and cell proliferation versus survival. HIF-1 is crucial for a variety of essential biological processes. HIF-1α expression and activity are regulated by major signal transduction pathways, including those involving phosphatidylinositol 3-kinase and extracellular regulated kinas/mitogen activated protein kinase. Although the number of patients reported in our study is small, the paired study design and the rigorous statistical comparisons used provide some confidence that the results are meaningful. A greater number of subjects are needed to support these differences; in addition, our study was limited by investigating only congenital giant naevi. Further studies on common small naevi would be of interest and might yield different findings.

''Although the number of patients reported in our study is small, the paired study design and the rigorous statistical comparisons used provide some confidence that the results are meaningful''

Comparison between the unaffected nearby normal skin of patients with GHN and normal control skin generated a list of 36 genes with increased expression and five with decreased expression. There were strong increases in melanoma associated gene (GenBank accession number, XM_056455) and SPARC-like 1 (SPARCL1; GenBank accession number, X86693; also known as MAST9 or hevin) expression. SPARC is strongly expressed in bone tissue, is distributed widely in many other tissues and cell types, and is associated generally with tissue remodelling—for example, it is abundant in tissues undergoing morphogenesis, mineralisation, angiogenesis, and pathological responses to injury and tumorigenesis. Experiments in vitro have provided evidence that SPARC disrupts cell adhesion, promotes changes in cell shape, inhibits the cell cycle, regulates cell differentiation, inactivates cellular responses to certain growth factors, and regulates extracellular matrix and matrix metalloprotease production. SPARC plays a role in angiogenesis, tumorigenesis, cataractogenesis, and wound healing.[23] The expression of genes for histone acetyltransferase p300 and cAMP responsive element binding protein (CBP; GenBank accession number, U65093) were increased. These proteins are required for the execution of crucial biological functions such as proliferation, differentiation, and apoptosis. Both proteins are believed to regulate the activity of a large number of general and cell specific transcription factors. One consequence of p300 depletion is transcriptional down-regulation of the cyclin E gene, caused by deacetylation of histones at its promoter, leading to activation of senescence checkpoints in the cell cycle.[24]

At the present time, the pathogenesis of GHN is not understood at the molecular level. There are clearly substantial differences between these giant naevi and the much more common small hereditary naevi, and between these and common naevi acquired during life. There are also differences in the biological behaviour of GHN among individuals, the most striking of which is the development of malignant melanoma in a small number of patients. It is hoped that the analysis of gene expression profiles may begin to provide data that will be useful in increasing our understanding of the biology of these lesions and the problems that they present.

Take home messages

- Gene expression profiling using DNA microarray technology showed that there was increased expression of 22 genes and decreased expression of 73 genes in giant hairy naevi (GHN) compared with nearby normal skin
- There was increased expression of 36 genes and decreased expression of five genes in normal skin near GHN compared with normal control skin
- Affected genes were those encoding structural proteins, proteins related to developmental processes, cell death associated proteins, transcription factors, growth factors, stress response modulators, and collagen associated proteins
- Thus, genetic profiles of GHN may provide insight into their pathogenesis, including their potential for malignant transformation

ACKNOWLEDGEMENTS

This study was supported by Shriners Hospitals for Children Grants 8660 and 8490, and National Institutes of Health Grants 1P50GM60338-1 and 5RO1GM572903.

Authors' affiliations
M R K Dasu, R E Barrow, R L McCauley, Department of Surgery, University of Texas Medical Branch, Galveston, TX 77550, USA
H K Hawkins, Department of Pathology, University of Texas Medical Branch

REFERENCES

1 **Penman HG**, Stringer HC. Malignant transformation in giant congenital pigmented nevus. Death in early childhood. *Arch Dermatol* 1971;**103**:428–32.
2 **Kopf AW**, Bart RS, Hennessey P. Congenital nevocytic nevi and malignant melanomas. *J Am Acad Dermatol* 1979;**1**:123–30.
3 **Jerdan MS**, Cohen BA, Smith RR, *et al*. Neuroectodermal neoplasms arising in congenital nevi. *Am J Dermatopathol* 1985;**7**(suppl):41–8.
4 **Block LI**, Conway H. Giant nevus of face and neck—excision and skin grafting. *Plast Reconstr Surg* 1963;**31**:472–7.
5 **Russell JL**, Reyes RG. Giant pigmented nevi. *JAMA* 1959;**171**:2083–6.
6 **Greeley PW**, Middleton AG, Curtin JW. Incidence of malignancy in giant pigmented nevi. *Plast Reconstr Surg* 1965;**36**:26–37.
7 **Reed WB**, Becker SW Jr, Nickei WR. Giant pigmented nevi, melanoma, and leptomeningeal melanocytosis. A clinical and histopathological study. *Arch Dermatol* 1965;**91**:100.
8 **Schleicher SM**, Lim SJ. Congenital nevi. *Int J Dermatol* 1995;**34**:825–9.
9 **Reed RJ**. Neuromesenchyme. The concept of a neurocristic effector cell for dermal mesenchyme. *Am J Dermatopathol* 1983;**5**:385–95.
10 **Hendrickson MR**, Ross JC. Neoplasms arising in congenital giant nevi: morphologic study of seven cases and a review of the literature. *Am J Surg Pathol* 1981;**5**:109–35.
11 **Carr KM**, Bittner M, Trent JM. Gene-expression profiling in human cutaneous melanoma. *Oncogene* 2003;**22**:3076–80.
12 **Loftus SK**, Pavan WJ. The use of expression profiling to study pigment cell biology and dysfunction. *Pigment Cell Res* 2000;**13**:141–6.
13 **Kim CJ**, Reintgen DS, Yeatman TJ. The promise of microarray technology in melanoma care. *Cancer Control* 2002;**9**:49–53.
14 **Chomczynski P**, Sacchi N. Single-step method of RNA isolation by acid guanidinium thiocyanate-phenol–chloroform extraction. *Anal Biochem* 1987;**162**:156–9.
15 **Spies M**, Dasu MR, Svrakic N, *et al*. Gene expression analysis in burn wounds of rats. *Am J Physiol Regul Integr Comp Physiol* 2002;**283**:R918–30.
16 **Li C**, Wong WH. Model-based analysis of oligonucleotide arrays: expression index computation and outlier detection. *Proc Natl Acad Sci U S A* 2001;**98**:31–6.

17 **Dudoit S**, Yang YH, Callow M, *et al*. Statistical methods for identifying differentially expressed genes in replicated cDNA microarray experiments. Berkely, CA: Department of Statistics, University of California at Berkely, Technical report 578.
18 **Spies M**, Chappell VL, Dasu MR, *et al*. Role of TNF-alpha in gut mucosal changes after severe burn. *Am J Physiol Gastrointest Liver Physiol* 2002;**283**:G703–8.
19 **Slominski A**, Costantino R, Howe J, *et al*. Molecular mechanisms governing melanogenesis in hamster melanomas: relative abundance of tyrosinase and catalase-B (gp 75). *Anticancer Res* 1991;**11**: 257–62.
20 **Guo J**, Cheng L, Wen DR, *et al*. Detection of tyrosinase mRNA in formalin-fixed, paraffin-embedded archival sections of melanoma, using the reverse transcriptase in situ polymerase chain reaction. *Diagn Mol Pathol* 1998;**7**:10–15.
21 **Hofbauer GF**, Kamarashev J, Geertsen R, *et al*. Tyrosinase immunoreactivity in formalin-fixed, paraffin-embedded primary and metastatic melanoma: frequency and distribution. *J Cutan Pathol* 1998;**25**:204–9.
22 **Bomirski A**, Slominski A, Bigda J. The natural history of a family of transplantable melanomas in hamsters. *Cancer Metastasis Rev* 1988;**7**:95–118.
23 **Yan Q**, Sage EH. SPARC, a matricellular glycoprotein with important biological functions. *J Histochem Cytochem* 1999;**47**:1495–506.
24 **Bandyopadhyay D**, Okan NA, Bales E, *et al*. Down-regulation of p300/CBP histone acetyltransferase activates a senescence checkpoint in human melanocytes. *Cancer Res* 2002;**62**:6231–9.